Stoch Environ Res Risk Assess
DOI 10.1007/s00477-013-0723-0

ORIGINAL PAPER

Assessing the effect of climate change on reference evapotranspiration in China

Dan Zhang · Xiaomang Liu · Haoyuan Hong

© Springer-Verlag Berlin Heidelberg 2013

Abstract Reference evapotranspiration (ET_0) is a key parameter in hydrological and meteorological studies. In this study, the FAO Penman–Monteith equation was used to estimate ET_0, and the change in ET_0 was investigated in China from 1960 to 2011. The results show that a change point around the year 1993 was detected for the annual ET_0 series by the Cramer's test. For the national average, annual ET_0 decreased significantly ($P < 0.001$) by −14.35 mm/decade from 1960 to 1992, while ET_0 increased significantly ($P < 0.05$) by 22.40 mm/decade from 1993 to 2011. A differential equation method was used to attribute the change in ET_0 to climate variables. The attribution results indicate that ET_0 was most sensitive to change in vapor pressure, followed by solar radiation, air temperature and wind speed. However, the effective impact of change in climate variable on ET_0 was the product of the sensitivity and the change rate of climate variable. During 1960–1992, the decrease in solar radiation was the main reason of the decrease in ET_0 in humid region, while decrease in wind speed was the dominant factor of decreases in ET_0 in arid region and semi-arid/semi-humid region of China. Decrease in solar radiation and/or wind speed offset the effect of increasing air temperature on ET_0, and together led to the decrease in ET_0 from 1960 to 1992. Since 1993, the rapidly increasing air temperature was the dominant factor to the change in ET_0 in all the three regions of China, which led to the increase in ET_0. Furthermore, the future change in ET_0 was calculated under IPCC SRES A1B and B1 scenarios with projections from three GCMs. The results showed that increasing air temperature would dominate the change in ET_0 and ET_0 would increase by 2.13–10.77, 4.42–16.21 and 8.67–21.27 % during 2020s, 2050s and 2080s compared with the average annual ET_0 during 1960–1990, respectively. The increases in ET_0 would lead to the increase in agriculture water consumption in the 21st century and may aggravate the water shortage in China.

Keywords Reference evapotranspiration · Climate change · Trend · GCMs

1 Introduction

Reference evapotranspiration (ET_0) is a representation of the environmental demand for evapotranspiration under a certain underlying surface, which is an important parameter for agricultural activities and hydro-meteorological studies, such as design of irrigation and drainage systems, water resources management and irrigation scheduling (Ganji et al. 2006; Sentelhas et al. 2010; Zhang et al. 2011; Nazemi and Elshorbagy 2012). Changes in ET_0 are of great significance for agricultural water use planning and irrigation system management. One of the expected consequences of the global warming is that the increasing surface temperature should lead to the increase in evaporative demand. However, in the last decades, both observed pan-evaporation and reference evapotranspiration were

D. Zhang · X. Liu (✉)
Institute of Geographic Sciences and Natural Resources Research, Chinese Academy of Sciences, No. 11A, Datun Road, Chaoyang District, Beijing 100101, China
e-mail: liuxm@igsnrr.ac.cn

D. Zhang
University of Chinese Academy of Sciences, No.19A Yuquan Road, Beijing 100049, China

H. Hong
Jiangxi Provincial Meteorological Observatory, Jiangxi Meteorological Bureau, No.109 ShengfuBeier Road, Nanchang 330046, China

Published online: 31 March 2013

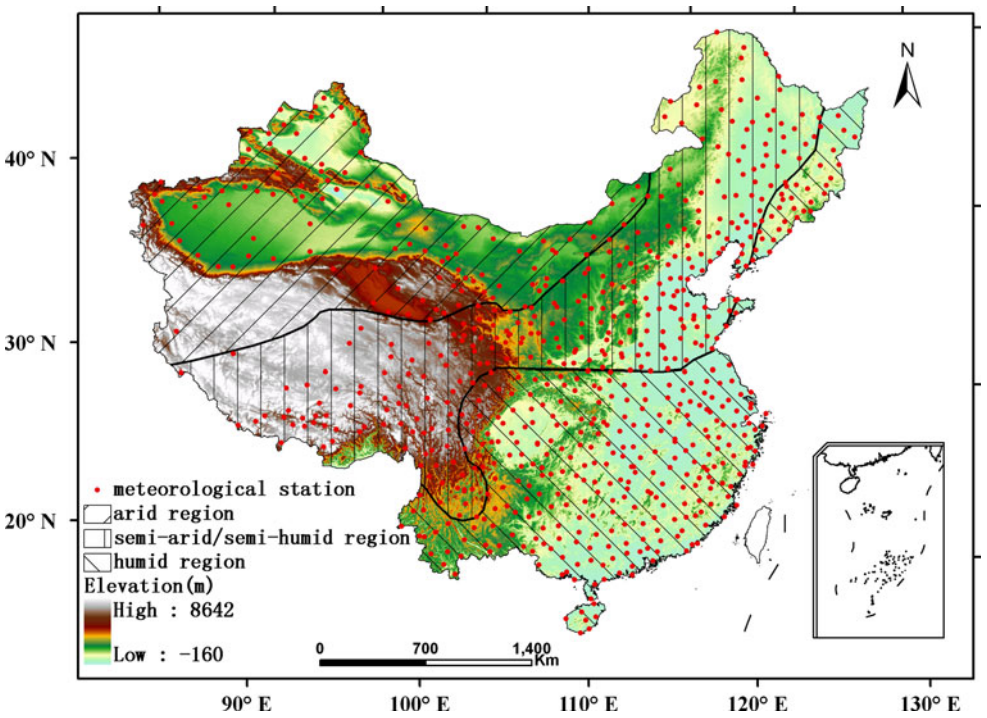

Fig. 1 The spatial distribution of the 653 meteorological stations in China. China was divided into three regions by the arid index

reported to have decreasing trends in different regions of the world (Brutsaert and Parlange 1998; Roderick and Farquhar 2002; Liu et al. 2004; Roderick et al. 2007; Zheng et al. 2009), which is known as "Evaporation Paradox" (Brutsaert and Parlange 1998).

The reasons of decreasing pan-evaporation and/or ET_0 have been widely discussed, and changes in climate variables such as air temperature, wind speed, solar radiation and vapor pressure were employed to explain the changes in pan-evaporation and/or ET_0. Some researchers revealed that decreasing wind speed was the dominating factor for decreasing ET_0 in many regions of the world, such as Australian (Roderick et al. 2007), Iran (Dinpashoh et al. 2011), Canada (Burn and Hesch 2007), Tibetan Plateau (Shenbin et al. 2006; Zhang et al. 2007; Liu et al. 2011) and the Haihe River basin (Zheng et al. 2009). Meanwhile, other researchers investigated that decreasing solar radiation was the main contributor to the decreasing ET_0 in Ireland (Stanhill and Möller 2008) and the Yangtze River basin (Xu et al. 2006; Wang et al. 2007). Water vapor and air temperature were also demonstrated as the dominating climate variable to the decreasing ET_0 in limited regions (Chattopadhyay and Hulme 1997; Speranskaya et al. 2001; Tabari et al. 2011).

In recent years, the changes in pan-evaporation and/or ET_0 were reported to have new dynamics. The increasing trends in pan-evaporation and/or ET_0 were detected in some regions in the world since 1990s. Zuo et al. (2011) detected that there was an abrupt change for annual ET_0 series in the Wei River basin of China around 1993, and ET_0 became to increase since 1993. Shadmani et al. (2012) found that increasing ET_0 was investigated in some cities in Iran in 1990s. Papaioannou et al. (2011) examined the trend in ET_0 in Greece, and found that annual ET_0 showed a declined trend from 1950 to the early 1980s and began to increase since the early 1980s.

In China, irrigation plays an important role in food security and roughly four fifths of grain harvest comes from irrigated land (Brown 2011; Gao et al. 2010). Considering the importance of changes in ET_0 for agricultural water use planning, the recent dynamics in ET_0 in China should be investigated, which was not available in the literature. The Penman–Monteith method recommended by Food and Agriculture Organization (FAO) is widely used to calculate ET_0 in China. The objectives of this study are (1) to characterize the changes in Penman–Monteith ET_0 in China from 1960 to 2011; (2) to investigate the reasons of changes in Penman–Monteith ET_0 in China; (3) to predict the responses of ET_0 to climate change from 2011 to 2099 under IPCC SRES A1B and B1 scenarios with projections from three GCMs.

2 Data

Daily meteorological records of 653 national meteorological stations during 1960–2011 in China from the National Climatic Centre of China Meteorological Administration

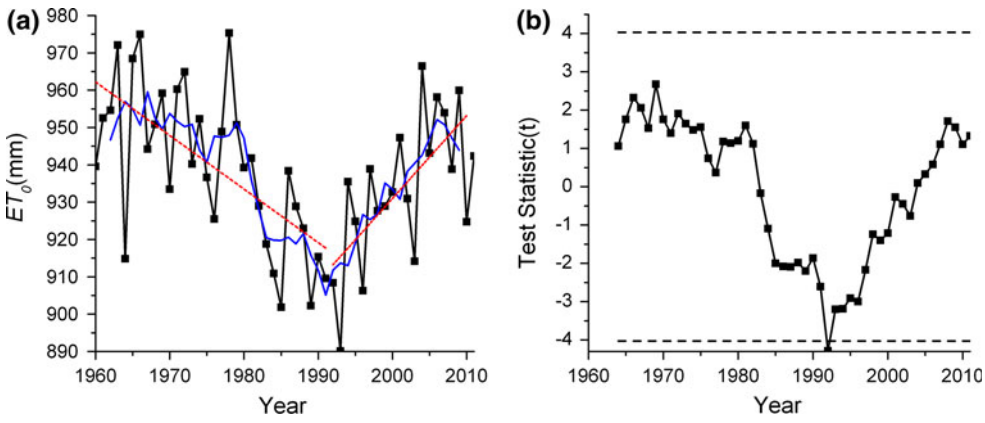

Fig. 2 Changes in reference evapotranspiration (**a**) and the Cramer's test for detecting a change in annual ET_0 (**b**) in China from 1960 to 2011. The *blue line* shows the 5 year moving average and the *red line* is the linear trends fitted to the period

(http://cdc.cma.gov.cn) were used in the study (Fig. 1). The data included daily precipitation, daily air temperatures (T_a) at 2 m height, wind speed measured at 10 m height, vapor pressure (VP) at 2 m height and sunshine duration. Wind speed (U) was adjusted to 2 m height using Allen et al. (1998) wind profile relationship to calculate ET_0. Sunshine duration of a day is defined as the sum of hours for which the direct solar irradiance exceeds 120 W/m^2 (WMO 1996). China was divided into three climatic regions based on the distribution of arid index (ϕ), which is the ratio between annual mean potential evapotranspiration and annual mean precipitation. The three climatic regions include arid region ($\phi \geq 4.0$), semi-arid/semi-humid region ($4.0 > \phi \geq 1.0$) and humid region ($\phi < 1.0$) (Ponce et al. 2000).

The WCRP (World Climate Research Programme) CMIP3 (Coupled Model Intercomparison Project) Multi-model data (monthly) was employed to predict the change in ET_0 from 2011 to 2099. Three consecutive 30 year, including 2011–2039(2020s), 2040–2069(2050s) and 2070–2099(2080s), were used to estimate the change in climate variables and ET_0 in the future. Two scenarios (SRES A1B and B1) were chosen for representing the different development patterns of the world. Three GCMs outputs were used as different future changes in climate variables: UKMO_HadCM3 with a resolution of 2.5° × 3.75°, MPI_ECHAM5 with a resolution of 2.8° × 2.8° and CCCMA_CGCM3.1 with a resolution of 3.7° × 3.7° (Meehl et al. 2007). All of the data was interpolated to 2.5° × 2.5° using inverse distance weighting. The GCM data were averaged over all grid cells whose centers lay in China.

3 Method

3.1 Statistical analysis

Cramer's test is performed to examine the stability of a record in terms of a comparison between the overall mean of an entire record and the means of certain parts of the record (e.g., Türkeş 1996). Cramer's test statistic t_k is calculated as:

$$t_k = \sqrt{\frac{n(N-2)}{N - n(1+\tau_k^2)}} \cdot \tau_k \tag{1}$$

$$\tau_k = \frac{\bar{x}_k - \bar{x}}{s},\ \bar{x}_k = \frac{1}{n}\sum_{i=k+1}^{k+n} x_i,\ \bar{x} = \frac{1}{N}\sum_{i=1}^{N} x_i \tag{2}$$

$\bar{x}$ and s are the mean and standard deviation of the entire period of N years, respectively, and $\bar{x}_k$ is the mean of the sub-period of n years to be compared with $\bar{x}$. The test statistic t_k is distributed as Student's t with (N-2) degrees of freedom. The null hypothesis of no significant difference between the mean of a sub-period and the mean of a whole period is rejected with the two-tailed test for large values of$|t_k|$.

The rank-based non-parametric Mann–Kendall statistical test (Mann 1945; Kendall 1975) has been commonly used for trend detection due to its robustness for non-normally distributed data, which are frequently encountered in

Table 1 Trend in associated climate variables and ET_0 in regions

Region	ET_0	T_a	U	VP	R_S
Period: 1960–1992					
Nation	−14.35***	0.11*	−0.07***	−0.01	−0.21***
Arid region	−11.66*	0.23**	−0.09***	0.04	−0.04
Semi-arid/Semi-humid	−9.82*	0.16*	−0.06**	0.03	−0.14***
Humid region	−19.33***	0.01	−0.08***	−0.06	−0.33***
Period: 1993–2011					
Nation	22.40*	0.50**	−0.06***	0.00	−0.04
Arid region	35.34**	0.66**	0.01	−0.09	0.06
Semi-arid/Semi-humid	10.94	0.44*	−0.10***	0.01	−0.16*
Humid region	28.02**	0.50**	−0.04*	0.01	0.04

Slope is the linear trend estimated by the linear regression. The slope unit of ET_0, T_a, U, VP and R_S is mm/decade, °C/decade, m s^{-1}/decade, kPa/decade and MJ m^{-2} day^{-1}/decade. *$P < 0.05$; **$P < 0.01$; ***$P < 0.001$

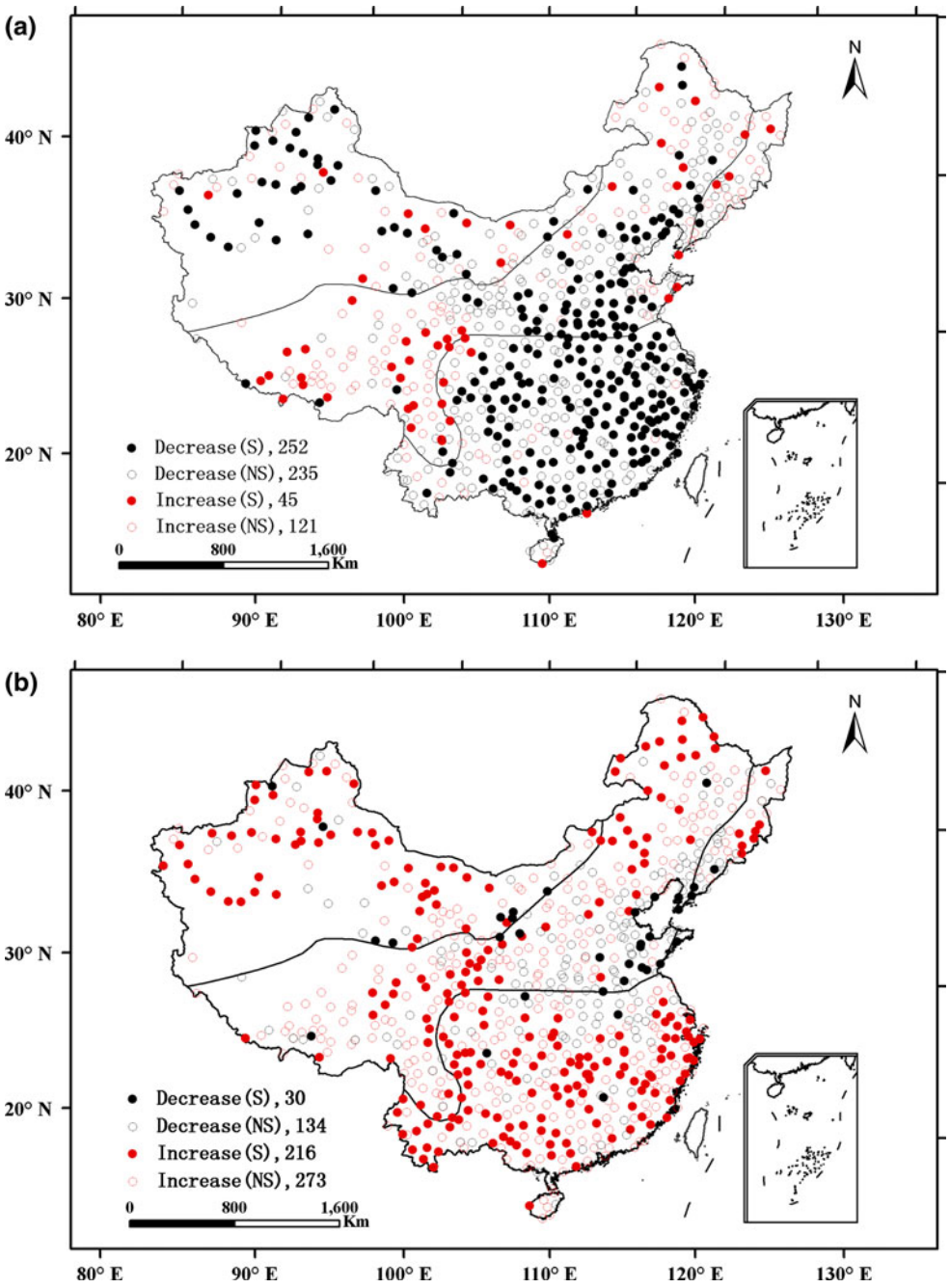

Fig. 3 Trends in annual ET_0 for the 653 meteorological stations in China during the period **a** 1960–1992 and **b** 1993–2011. *S* and *NS* in the figure legend indicate significance and insignificance at $P = 0.05$, respectively. The *numbers* given after S or NS indicate the number of stations out of 653 stations in these categories

hydro-climatic time-series (e.g., Zheng et al. 2009; Liu and Zhang 2012). By assuming a normal distribution at the significant level of $P = 0.05$, a positive Mann-Kendal statistics Z larger than 1.96 indicates an significant increasing trend, while a negative Z lower than -1.96 indicates a significant decreasing trend. Critical Z values of ± 1.64, ± 2.58 and ± 3.29 were used for the probabilities of $P = 0.1$, 0.01 and 0.001, respectively. The trend of ET_0 and climate variables from the 1960 to 2011 was determined by linear regression while the Mann–Kendall test was conducted to determine whether the slope of the regression line is significant.

3.2 Reference evapotranspiration

The Penman–Monteith ET_0 formula (Allen R et al. 1998) is expressed as:

$$ET_0 = \frac{0.408\Delta(R_n - G) + \gamma \frac{900}{T_a+273} U \cdot (VP_s - VP)}{\Delta + \gamma(1 + 0.34U)} \quad (3)$$

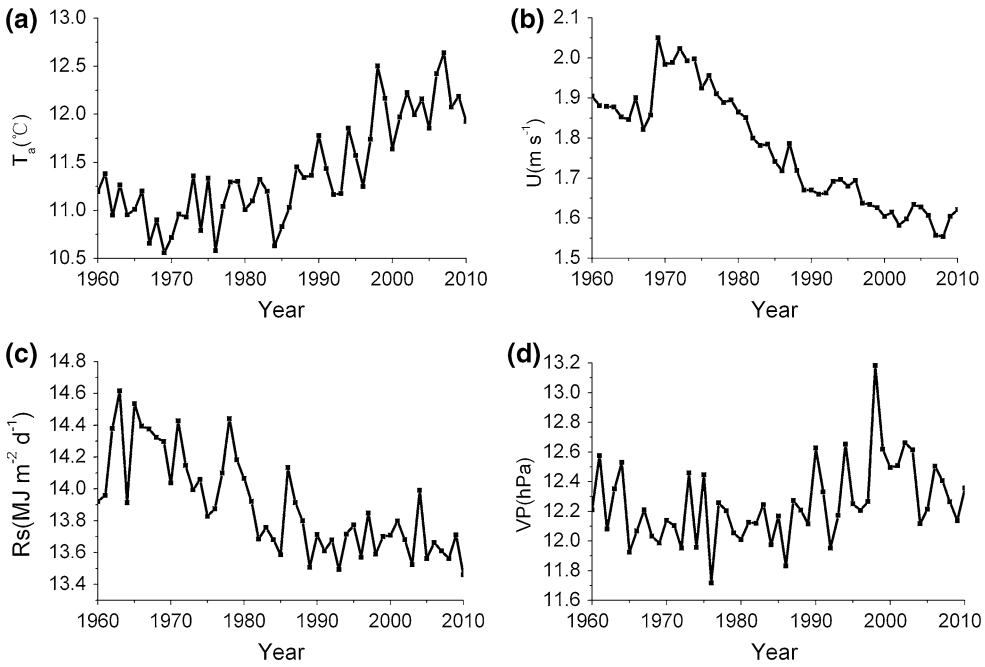

Fig. 4 Variations of **a** air temperature, **b** wind speed, **c** solar radiation and **d** vapor pressure for the national average from 1960 to 2011

where R_n is net radiation at reference surface (MJ m^{-2} day^{-1}), G is soil heat flux density (MJ m^{-2} day^{-1}), T_a is daily mean temperature (°C), U is the wind speed at 2 meters height (m s^{-1}), VP_s is saturated vapor pressure (kPa), VP is actual vapor pressure (kPa), Δ is the slope of vapor pressure curve versus temperature (kPa °C^{-1}) and γ is psychrometric constant (kPa °C^{-1}). R_n represents the difference between net shortwave radiation (R_{ns}) and net long-wave radiation (R_{nl}). R_{nl} was estimated by a function of temperature, actual vapor pressure and sunshine duration (Allen R et al. 1998). Regional averages of ET_0 and climate variables were first calculated by averaging the values of stations included in the region. Temporal trends and change points of the average ET_0 and climate variables were then quantified by the linear regression and the Cramer's test, respectively.

3.3 Sensitivity coefficient

Sensitive coefficient was defined as the ratio of change rate of ET_0 and change rate of meteorological factor in this study (McCuen 1974):

$$S(x_i) = \lim_{\Delta x_i/x_i} \left(\frac{\Delta ET_0/ET_0}{\Delta x_i/x_i}\right) = \frac{\partial ET_0}{\partial x_i} \times \frac{x_i}{ET_0} \quad (4)$$

where x_i is the meteorological factor; S_{xi} is the sensitivity coefficient of ET_0 related to x_i which is a non-dimensional form. This pattern can be easily used for comparison of different meteorological factors. Essentially, a positive/negative sensitivity coefficient of a meteorological factor indicates that ET_0 will increase/decrease with the meteorological factor increasing. The larger absolute value of the sensitivity coefficient, the larger effect a given meteorological factor has on ET_0.

3.4 Attribution assessment

For attribution, the change in ET_0 can be approximately estimated by the following differentiating equation (Zheng et al. 2009):

$$\frac{dET}{dt} = \frac{\partial ET}{\partial R_s}\frac{dR_s}{dt} + \frac{\partial ET}{\partial T_a}\frac{dT_a}{dt} + \frac{\partial ET}{\partial U}\frac{dU}{dt} + \frac{\partial ET}{\partial VP}\frac{dVP}{dt} + \delta \quad (5(a))$$

or simplified as:

$$L\_(ET_0) = C\_(R_s) + C\_(T_a) + C\_(U) + C\_(VP) + \delta \quad (5(b))$$

where $L\_(ET_0)$ is the calculated long term trend in ET_0 by linear regression. $C\_(R_s)$, $C\_(T_a)$, $C\_(U)$ and $C\_(VP)$ are individual contributions to the trends in ET_0 due to the change in R_s, T_a, U and VP, respectively. The sum of $C\_(R_s)$, $C\_(T_a)$, $C\_(U)$ and $C\_(VP)$ is simplified as $C\_(ET_0)$. δ is the error item between $L\_(ET_0)$ and $C\_(ET_0)$. Furthermore, the individual relative contribution of climate variable to the trend in ET_0 can be estimated as:

$$RC\_(x_i) = \frac{C\_(x_i)}{L\_ET_0} \times 100\% \quad (6)$$

where $RC\_(x_i)$ is the relative contribution of the climate variable x_i.

Table 2 Sensitivity coefficients of ET_0 to climate variables

Region	S(T_a) Period: 1960–1992	S(U)	S(R_s)	S(VP)	S(T_a) Period: 1993–2011	S(U)	S(R_s)	S(VP)
Nation	0.37	0.18	0.42	−0.70	0.37	0.19	0.42	−0.63
Arid region	0.14	0.27	0.27	−0.47	0.15	0.27	0.29	−0.42
Semi-arid/Semi-humid	0.20	0.20	0.36	−0.63	0.21	0.21	0.36	−0.58
Humid region	0.61	0.12	0.51	−0.84	0.59	0.13	0.51	−0.75

4 Results

4.1 Changes in ET_0

Figure 2a shows the variation of annual ET_0 averaged by the 653 meteorological stations in China from 1960 to 2011. A change point for annual ET_0 series was detected around the year 1993 by Cramer's test (Fig. 2b). Annual ET_0 decreased significantly ($P < 0.001$) by 14.35 mm/decade from 1960 to 1992, while ET_0 increased significantly ($P < 0.05$) by 22.40 mm/decade from 1993 to 2011. For the three climatic regions, change points for annual ET_0 were also identified by Cramer's test around 1993 (Table 1). In arid region, annual ET_0 decreased significantly ($P < 0.05$) by −11.66 mm/decade before 1993 while increased significantly ($P < 0.01$) by 35.34 mm/decade after 1993. In semi-arid/semi-humid region, annual ET_0 decreased significantly ($P < 0.05$) by −9.82 mm/decade before 1993 but increased insignificantly ($P > 0.1$) after 1993. In humid region, ET_0 decreased significantly ($P < 0.001$) by −19.33 mm/decade before 1993 while increased significantly ($P < 0.01$) by 28.02 mm/decade. Figure 3a shows the spatial distribution of trends in annual ET_0 at the 653 meteorological stations before and after 1993. During the period 1960–1992, annual ET_0 showed a decreasing trend at 487 stations and the decreasing trends were significant ($P < 0.05$) at 252 stations. During the period 1993–2011(Fig. 3b), annual ET_0 increased at 479 stations and the increasing trends were significant ($P < 0.05$) at 216 stations.

4.2 Changes in climate variables

Figure 4 and Table 1 show the variations of climate variables in China from 1960 to 2011. T_a increased significantly ($P < 0.05$) by 0.11 °C/decade from 1960 to 1992, while T_a increased significantly ($P < 0.01$) by 0.50 °C/decade from 1993 to 2011 for the China average. The similar trends in T_a were also found in the three climatic regions, and the increasing trend in T_a from 1993 to 2011 was about 50 times as that from 1960 to 1992 in humid region. U decreased significantly ($P < 0.001$) by −0.07 and −0.06 m s^{-1}/decade before and after 1992 for the China average. The change in U was spatially uneven, the decreasing trends in U slowed in arid and humid regions while accelerated in semi-arid/semi-humid region since 1993. R_s decreased significantly ($P < 0.001$) by −0.21 MJ m^{-2} day^{-1}/decade from 1960 to 1992, while T_a decreased insignificantly ($P > 0.1$) from 1993 to 2011 for the China average. T_a even showed increasing trend in arid and humid regions from 1993 to 2011 (termed 'from dimming to brightening'). The changing trend in VP was not significant ($P > 0.1$) both from 1960 to 1992 and from 1993 to 2011.

4.3 Sensitivity of ET_0 to climate variables

Sensitivity coefficients were calculated by Eq. (4) and the results was shown in Table 2. During the period 1960–1992, the mean annual sensitivity coefficients of ET_0 to T_a, U, R_s and VP for China average were 0.37, 0.18, 0.42 and −0.70, respectively. It indicates that 10 % increase in

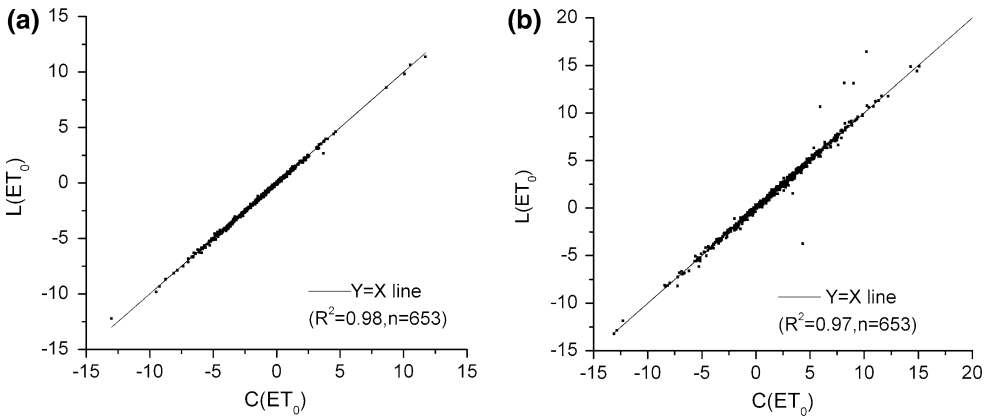

Fig. 5 Comparison between the calculated ET_0 trend $C(ET_0)$ and the detected ET_0 trend $L(ET_0)$ by linear regression in China **a** from 1960 to 1992 **b** from 1993 to 2011

Table 3 Contributions of climate variables to the long term trend in ET_0

Region	$C\_(T_a)$	$C\_(U)$	$C\_(VP)$	$C\_(R_S)$	C_ET_0	L_E_{pan}	ε	$\rho(\varepsilon)(\%)$
Period: 1960–1992								
Nation	0.14	−0.73	−0.02	−0.77	−1.38	−1.44	−0.04	2.91
Arid region	0.55	−1.55	−0.04	−0.05	−1.09	−1.17	−0.07	6.34
Semi-arid/Semi-humid	0.37	−0.68	−0.24	−0.40	−0.95	−0.98	−0.02	2.48
Humid region	−0.21	−0.49	0.17	−1.36	−1.89	−1.93	−0.05	2.38
Period: 1993–2011								
Nation	2.99	−0.37	−0.23	−0.17	2.22	2.24	0.03	1.20
Arid region	3.36	0.31	−0.24	0.12	3.55	3.53	−0.02	−0.61
Semi-arid/Semi-humid	2.68	−0.80	−0.12	−0.63	1.13	1.09	−0.03	−2.37
Humid region	3.13	−0.23	−0.31	0.13	2.72	2.80	0.09	3.24

T_a, U and R_s would result in 3.7, 1.8 and 4.2 % increase in ET_0, while 10 % increase in VP could result in 7.0 % decrease in ET_0. The sensitivity coefficients of ET_0 to climate variables from 1993 to 2011 nearly kept the same as that from 1960 to 1992. In the past 50 years, ET_0 was most sensitive to change in VP for China average, followed by R_s, T_a and U. For the three climatic regions, the order was VP, R_s, U and T_a in arid region and semi-arid/semi-humid region, while it was VP, T_a, R_s and U in humid region.

4.4 Attribution of changes in ET_0

The contributions of climate variables to the change in ET_0 were estimated according to Eqs. (5) and (6). As shown in Fig. 5, the calculated ET_0 trends $C\_(ET_0)$ fitted well with the detected ET_0 trends $L\_(ET_0)$ by linear regression with $R^2 = 0.98$ and 0.97 before and after the 1993 respectively. Table 3 shows the contribution of each climate variable to the trend in annual ET_0. During the period 1960–1992, the change in T_a, U, R_s and VP could have led to change in ET_0 by 0.14, −0.73, −0.77 and −0.02 mm/a, respectively. The combined effects of the four climate factors results in a decrease in ET_0 by −1.39 mm/a, and the absolute and relative error compared to the detected ET_0 trend was −0.04 mm/a and 2.91 % respectively. The increasing T_a would lead to the increase in ET_0, but the effect has been offset by the decreasing U and R_s from 1960 to 1992. During the period 1993–2011, the change in T_a, U, R_s and VP could have led to the change in ET_0 by 2.99, −0.37, −0.17 and −0.23 mm/a, respectively. The combined effects of the four climate variables resulted in an increase in ET_0 at 2.21 mm/a. The absolute and relative error compared to the detected ET_0 trend was 0.03 mm/a and 1.20 %, respectively. The increase in T_a was the dominant factor for the increase in ET_0 from 1993 to 2011. Due to the large amplitude of increased T_a, the positive effect of T_a offset the negative effect of U, R_s and VP to ET_0.

For the three climatic regions, the decreasing U was the dominant factor for the decrease in ET_0 in arid region and semi-arid/semi-humid region, while decreasing R_s was the dominant factor in humid region from 1960 to 1992 (Table 3). During 1993–2011, increasing T_a was the dominant factor for the increase in ET_0 in all the three regions. Figure 6 shows the spatial distribution of dominating climate variable for the change in ET_0 at the 653 stations in China before and after 1992. From 1960 to 1992, T_a, U and R_s were the dominant factor for the change in ET_0 at about 22, 33 and 41 % stations, respectively; while VP was the dominant factor at only about 4 % stations. Spatially, U was the dominant factor at most stations in arid region and semi-arid/semi-humid region, while R_s was the dominant factor in humid region from 1960 to 1992. From 1993 to 2011, T_a was the dominant factor leading to the change in ET_0 at about 62 % stations, and U was the dominant factor at about 24 % stations which mostly located in semi-arid/semi-humid region. VP and R_s were the dominant factor at about 11 and 3 % stations, respectively.

4.5 Responses to climate change in the future

To predict the ET_0 trend in the future, the relative change in ET_0 for the periods 2020s, 2050s and 2080s was estimated by the product of the sensitivity and the change rate of climate variable based on the outputs of three GCMs under IPCC SRES A1B and B1 emission scenarios, which should not adjust the differences between the observed data and the modeled data (Fig. 7; Table 4). The results show that changes in T_a and VP would be significantly, and changes in T_a and VP would dominate the change in ET_0. However, changes in U and R_s would be not significantly and the effects are not obvious. During 2020s, T_a would increase by 14.46–48.86 %, which would lead to the increase in ET_0 by 5.36–18.10 %. VP would increase by 14.46–48.86 %,

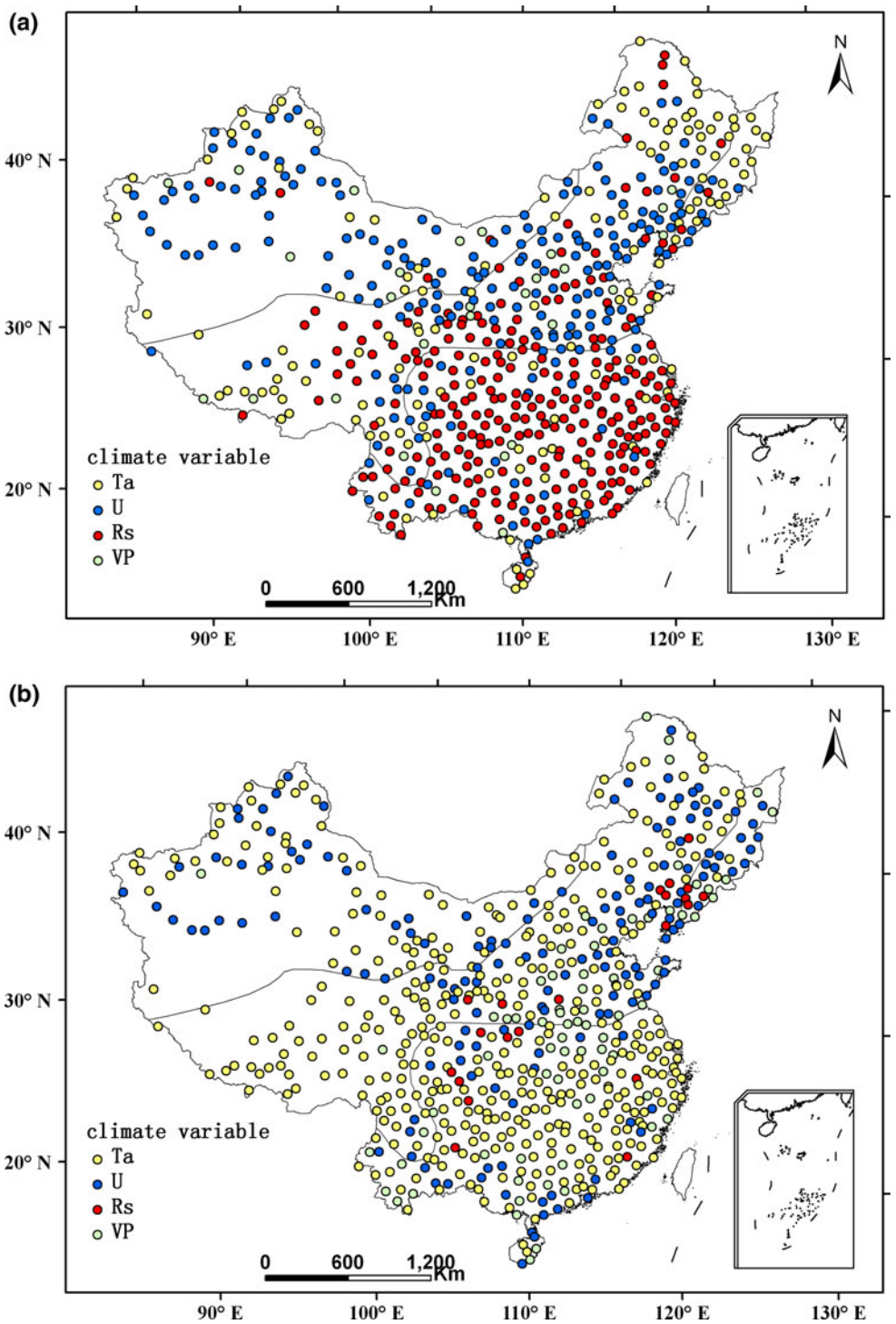

Fig. 6 Spatial distribution of dominating factor in China during the period 1960–1992(**a**) and 1993–2011(**b**)

which would lead to the decrease in ET_0 by 2.86–6.62 %. The four climate factors together would lead to the increase in ET_0 by 3.15–10.77 % during 2020s.

During 2050s, increase in T_a would lead to the increase in ET_0 by 11.81–28.75 %, while increase in *VP* would lead to the decrease in ET_0 by 7.32–11.64 %, and the four climate factors together would lead to the increase in ET_0 by 4.42–16.21 %. During 2080s, increase in T_a would lead to the increase in ET_0 by 18.88–37.58 %, while increase in *VP* would lead to the decrease in ET_0 by 10.26–18.41 %, and the four climate factors together would lead to the increase in ET_0 by 8.67–21.27 %. Increase in ET_0 would be more significantly under A1B scenario than that under B1 scenario because the increase in T_a is more significantly

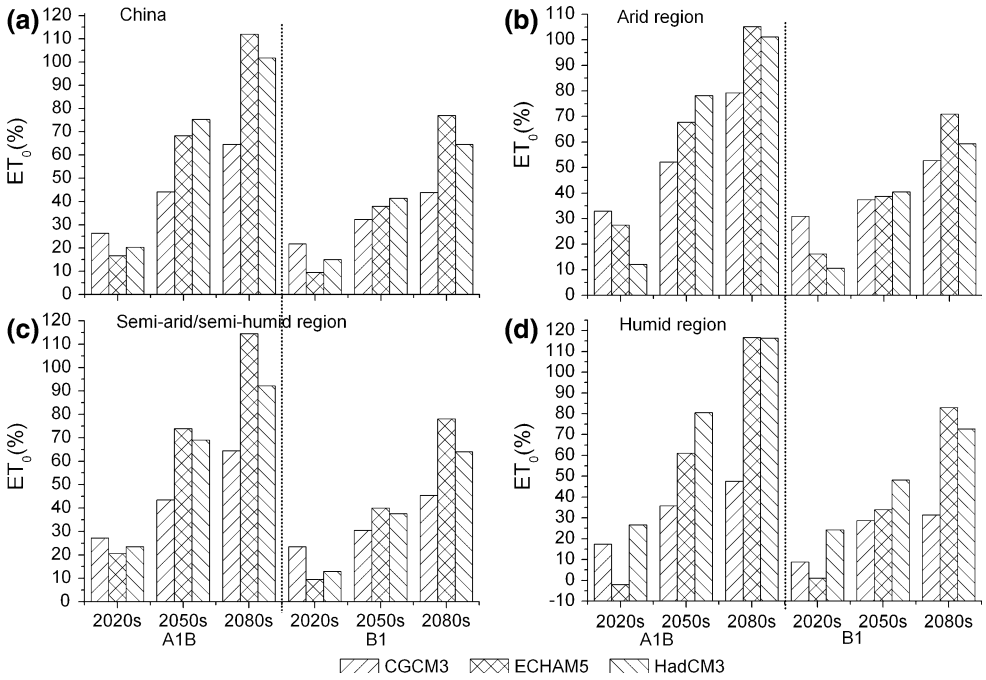

Fig. 7 Changes in ET_0 of three GCMs in the future under A1B and B1 scenarios **a** for the whole China, **b** for the arid region, **c** for the semi-arid/semi-humid region and **d** for the humid region

Table 4 Changes in climate variables of three GCMs in the future under A1B and B1 scenarios (%)

GCMs	Scenario	T_a		U		R_s		VP		$C\_(ET_0)$
		Trend	$C\_(T_a)$	Trend	$C\_(U)$	Trend	$C\_(R_s)$	Trend	$C\_(VP)$	
2020s										
CGCM	A1B	48.86	18.10	−2.42	−0.45	−0.63	−0.26	10.47	−6.62	10.77
	B1	41.95	15.54	−2.70	−0.50	−0.32	−0.13	8.33	−5.27	9.64
ECHAM	A1B	17.97	6.66	−0.19	−0.04	−0.91	−0.38	4.89	−3.09	3.15
	B1	14.46	5.36	0.10	0.02	−0.92	−0.38	4.52	−2.86	2.13
HADCM	A1B	31.20	11.56	−0.88	−0.16	−0.78	−0.32	7.86	−4.97	6.10
	B1	24.33	9.01	0.16	0.03	−0.78	−0.32	5.63	−3.56	5.15
2050s										
CGCM	A1B	77.58	28.75	−3.58	−0.66	−0.56	−0.23	18.39	−11.64	16.21
	B1	58.57	21.70	−2.32	−0.43	−0.63	−0.26	13.41	−8.49	12.52
ECHAM	A1B	46.81	17.34	−2.50	−0.46	1.83	0.76	15.44	−9.77	7.87
	B1	31.88	11.81	−0.60	−0.11	0.09	0.04	11.57	−7.32	4.42
HADCM	A1B	71.20	26.38	−5.12	−0.95	1.89	0.78	17.93	−11.35	14.87
	B1	48.33	17.91	−2.94	−0.54	0.22	0.09	12.89	−8.16	9.30
2080s										
CGCM	A1B	99.62	36.91	−4.82	−0.89	−0.02	−0.01	23.30	−14.75	21.27
	B1	71.44	26.47	−2.41	−0.45	−0.06	−0.02	16.22	−10.26	15.74
ECHAM	A1B	71.59	26.52	−1.63	−0.30	2.89	1.20	24.70	−15.63	11.79
	B1	50.94	18.88	−0.24	−0.05	1.91	0.79	17.30	−10.95	8.67
HADCM	A1B	101.44	37.58	−6.44	−1.19	1.56	0.65	29.08	−18.41	18.63
	B1	69.68	25.82	−4.22	−0.78	0.94	0.39	19.25	−12.19	13.24

under A1B scenario. In addition, the increase in annual ET_0 predicted by ECHAM5 was generally higher than that by HadCM3 and CGCM3.

5 Discussion

5.1 Uncertainties

The differentiation equation method was used to quantify the contributions of climate variables to trends in ET_0. The errors between $C\_ ET_0$ and $L\_ ET_0$ could come from the assumption that the four climate variables (T_a, VP, U and R_s) were independent in the differentiation equation (Eq. (5)). However, the four climate variables impacted each other and they were not totally independent. In addition, the partial derivatives of ET_0 to climate variables were not constant but fluctuated during 1960–2011. The mean values of partial derivatives were used to calculate the contribution in Eq. (5), which may lead to uncertainties and errors. In addition, the VP was considered instead of vapor pressure deficit in our study which was different from Roderick et al. (2007), because vapor pressure deficit is the difference between saturation water vapor (VPs) and VP, where VPs is a function of air temperature.

Uncertainties also exist in the evaluation of changes in ET_0 based on the outputs of GCMs. As presented by many researches, the largest uncertainty of climate projection and related impact assessment often comes from GCMs due to model structures (Shackley et al. 1998; Barnett et al. 2006; Kay et al. 2009). The prediction results calculated by different GCMs outputs had significant differences. For example, ET_0 would increase by 10.77 % based on the results of CGCM model under A1B scenarios, while ET_0 would increase by 3.15 % under the result of ECHAM model.

5.2 Compared with previous studies

The result of this study was compared with the previous studies in China. Xu et al. (2006) found that the pan evaporation and ET_0 in Yangtze River basin decreased from 1960 to 2000 which was mainly caused by the decrease in radiation. Cong et al. (2009) concluded that pan evaporation in China decreased from 1956 to 1985 which was mainly caused by decreasing radiation and wind speed while pan evaporation increased from 1986 to 2005 which was caused by decreasing vapor pressure deficit. Zheng et al. (2009) found that wind speed was the dominant factor contributing to pan evaporation decrease from 1957 to 2001 in the Haihe River basin, China. Most of the previous studies support our result of the change in ET_0 for different climatic regions in China. However, our result was partly different with the conclusion of Cong et al. (2009). They indicated that the decreasing vapor pressure deficit was the dominant factor to the increased pan evaporation from 1986 to 2005 in China. This was mainly due to the different estimation method of ET_0 and different change point of ET_0 series, etc.

6 Conclusion

In this study, the temporal change and attribution of climate variables to ET_0 were investigated in China based on 653 national meteorological stations during 1960–2011. A change point for ET_0 series was detected around the year 1993 by Cramer's test. ET_0 decreased significantly ($P < 0.001$) at -14.35 mm/decade from 1960 to 1992, while ET_0 increased significantly ($P < 0.05$) at 22.40 mm/decade from 1992 to 2011. Before 1993, T_a increased significantly ($P < 0.05$). VP decreased insignificantly ($P > 0.1$) while U and R_s decreased significantly ($P < 0.001$). After 1993, T_a increased significantly ($P < 0.01$) and VP increased insignificantly ($P > 0.1$). While U decreased significantly ($P < 0.001$) and R_s decreased insignificantly ($P > 0.1$).

Meanwhile, the sensitivity of ET_0 to climate variables was analyzed. In the past 50 years, sensitivity coefficients were relative stable. VP was the most sensitive climate variable in China, follow by R_s, T_a and U. A differentiation equation method was used to attribute the change in ET_0 to climate variables. The proportional contributions of T_a, U, R_s and VP to the trend in ET_0 were -9.66, 51.07, 53.99 and 1.69 % during the period 1960–1992, respectively. It meant that the positive effect of T_a had been offset by the decreasing U and R_s. ET_0 was dominated by R_s in humid region, while dominated by U in arid and semi-arid regions. However, the proportional contributions of T_a, U, R_s and VP to the increased ET_0 were 133.35, -16.61, -7.77 and -10.17 % during the period 1992–2011, respectively. It can be inferred that the increase in T_a was the dominant factor for the increase in ET_0 in China.

To predict the change in ET_0 in the future, ET_0 was estimated under IPCC SRES A1B and B1 scenarios by three GCMs. The results showed that the changing amplitude of climate variables and ET_0 under A1B scenario would be larger than under B1 scenario at the same period. T_a and VP would be increasing rapidly in the future which would be the main factors impacting on ET_0 would increase from 9.47 to 26.37, 32.25–72.31 and 43.87–111.96 mm by three GCMs during 2020s, 2050s and 2080s, respectively.

Acknowledgments This research was supported by the "Strategic Priority Research Program-Climate Change: Carbon Budget and Relevant Issues" of the Chinese Academy of Sciences (Grant No. XDA05090309) and National Basic Research Program of China (2010CB428403).

References

Allen R G, Pereira L S, Raes D and Smith M (1998) Crop evapotranspiration-Guidelines for computing crop water requirements-FAO Irrigation and drainage paper 56. FAO, Rome, 300: 6541

Barnett DN, Brown SJ, Murphy JM, Sexton DMH, Webb MJ (2006) Quantifying uncertainty in changes in extreme event frequency in response to doubled CO_2 using a large ensemble of GCM simulations. Clim Dynam 26(5):489–511

Brown LR (2011) World on the edge: how to prevent environmental and economic collapse. WW Norton & Co Inc

Brutsaert W, Parlange M (1998) Hydrologic cycle explains the evaporation paradox. Nature 396:30. doi:10.1038/23845

Burn DH, Hesch NM (2007) Trends in evaporation for the Canadian Prairies. J Hydrol 336(1):61–73

Chattopadhyay N, Hulme M (1997) Evaporation and potential evapotranspiration in India under conditions of recent and future climate change. Agric Forest Meteorol 87(1):55–73

Cong Z, Yang D, Ni G (2009) Does evaporation paradox exist in China? Hydrol Earth Syst Sci 13(3):357

Dinpashoh Y, Jhajharia D, Fakheri-Fard A, Singh VP, Kahya E (2011) Trends in reference crop evapotranspiration over Iran. J Hydrol 399:422–433

Ganji A, Ponnambalam K, Khalili D, Karamouz M (2006) Grain yield reliability analysis with crop water demand uncertainty. Stoch Environ Res Risk Assess 20(4):259–277

Gao C, Gemmer M, Zeng XF, Liu B, Su BD, Wen YH (2010) Projected streamflow in the Huaihe River Basin (2010–2100) using artificial neural network. Stoch Environ Res Risk Assess 24(5):685–697

Kay A, Davies H, Bell V, Jones R (2009) Comparison of uncertainty sources for climate change impacts: flood frequency in England. Clim Change 92(1):41–63

Kendall M (1975) Rank correlation measures. Charles Griffin, London 202

Liu X, Zhang D (2012) Trend analysis of reference evapotranspiration in Northwest China: the roles of changing wind speed and surface air temperature. Hydrol Process. doi:10.1002/hyp.9527

Liu B, Xu M, Henderson M, Gong W (2004) A spatial analysis of pan evaporation trends in China, 1955–2000. J Geophys Res 109:D15102

Liu X, Zheng H, Zhang M, Liu C (2011) Identification of dominant climate factor for pan evaporation trend in the Tibetan Plateau. J Geogr Sci 21(4):594–608

Mann HB (1945) Non-parametric tests against trend. Econometrica 13:245–259

McCuen RH (1974) A sensitivity and error analysis cf procedures used for estimating evaporation. J Am Water Resour As 10(3):486–497

Meehl G, Covey C, Delworth T, Latif M, McAvaney B, Mitchell J, Stouffer R, Taylor K (2007) The WCRP CMIP3 Multimodel Dataset: a new era in climate change research. BAMS 88:1383–1394. doi:10.1175,BAMS-88-9-1383

Nazemi A, Elshorbagy A (2012) Application of copula modelling to the performance assessment of reconstructed watersheds. Stoch Environ Res Risk Assess 26(2):189–205

Papaioannou G, Kitsara G and Athanasatos S (2011) Impact of global dimming and brightening on reference evapotranspiration in Greece. J Geophys Res, 116(D9): D09107

Ponce VM, Pandey RP, Ercan S (2000) Characterization of drought across climatic spectrum. J Hydrol Eng 5(2):222–224

Roderick ML, Farquhar GD (2002) The cause of decreased pan evaporation over the past 50 years. Science 298(5597):1410–1411

Roderick ML, Rotstayn LD, Farquhar GD, Hobbins MT (2007) On the attribution of changing pan evaporation. Geophys Res Lett 34:L17403

Sentelhas PC, Gillespie TJ, Santos EA (2010) Evaluation of FAO Penman–Monteith and alternative methods for estimating reference evapotranspiration with missing data in Southern Ontario Canada. Agric Water Manage 97(5):635–644

Shackley S, Young P, Parkinson S, Wynne B (1998) Uncertainty, complexity and concepts of good science in climate change modelling: are GCMs the best tools? Clim Change 38(2):159–205

Shadmani M, Marofi S, Roknian M (2012) Trend analysis in reference evapotranspiration using Mann–Kendall and Spearman's rho tests in arid regions of Iran. Water Resour Manag 26(1):211–224

Shenbin C, Yunfeng L, Thomas A (2006) Climatic change on the Tibetan Plateau: potential evapotranspiration trends from 1961–2000. Clim Change 76(3):291–319

Speranskaya NA, Zhuravin SA, Mennel MJ (2001) Evaporation changes over the contiguous United States and the former USSR: a reassessment. Geophys Res Lett 28(13):2665–2668

Stanhill G, Möller M (2008) Evaporative climate change in the British Isles. Int J Climatol 28(9):1127–1137

Tabari H, Marofi S, Aeini A, Talaee PH, Mohammadi K (2011) Trend analysis of reference evapotranspiration in the western half of Iran. Agr Forest Meteorol 151(2):128–136

Türkeş M (1996) Spatial and temporal analysis of annual rainfall variations in Turkey. Int J Climatol 16(9):1057–1076

Wang Y, Jiang T, Bothe O, Fraedrich K (2007) Changes of pan evaporation and reference evapotranspiration in the Yangtze River basin. Theor Appl Climatol 90(1):13–23

WMO (1996), Guide to Meteorological Instruments and Methods of Observation. 6th ed. WMO Rep. 8, World Meteorological Organization, Geneva, Switzerland

Xu C, Gong L, Jiang T, Chen D, Singh V (2006) Analysis of spatial distribution and temporal trend of reference evapotranspiration and pan evaporation in Changjiang (Yangtze River) catchment. J Hydrol 327(1):81–93

Zhang Y, Liu C, Tang Y, Yang Y (2007) Trends in pan evaporation and reference and actual evapotranspiration across the Tibetan Plateau. J Geophys Res 112:D12110

Zhang QA, Xu CY, Chen YD, Ren LL (2011) Comparison of evapotranspiration variations between the Yellow River and Pearl River basin China. Stoch Environ Res Risk Assess 25(2):139–150

Zheng H, Liu X, Liu C, Dai X and Zhu R (2009) Assessing contributions to panevaporation trends in Haihe River Basin China. J Geophys Res, 114(D24): D24105

Zuo D, Xu Z, Yang H, Liu X (2011) Spatiotemporal variations and abrupt changes of potential evapotranspiration and its sensitivity to key meteorological variables in the Wei River basin China. Hydrol Process 26(8):1149–1160